Dura, JL.; Solanes, C.; De Andres, J.; Saiz Rodríguez, FJ. (2022). Effect of Lead Position and Polarity on Paresthesia Coverage in Spinal Cord Stimulation Therapy: A Computational Study. Neuromodulation: Technology at the Neural Interface. 25(5):680-692. https://doi.org/10.1016/j.neurom.2021.12.013

Effect of Lead Position and Polarity on Paresthesia Coverage in Spinal Cord Stimulation Therapy: A Computational Study

Jose L. Dura, MEng[1]; Carmen Solanes, PhD[1]; Jose De Andres, MD, PhD[2,3]; Javier Saiz, PhD[1]

[1] Center of Research and Innovation in Bioengineering, Universitat Politècnica de València, València, Spain;
[2] Anesthesia, Critical Care, and Multidisciplinary Pain Management Department, General University Hospital, València, Spain; and
[3] Anesthesia Unit, Surgical Specialties Department, Valencia University Medical School, València, Spain

ABSTRACT

Objectives: The effect of lead placement and programming strategies on spinal cord stimulation (SCS) therapy has been widely studied; however, there is a need to optimize these parameters to favor dorsal column (DC) over dorsal root (DR) stimulation in complex pain treatment. This study aimed to determine the optimal lateral distance between two leads and the effect of transverse stimulation using a mathematical model.

Materials and Methods: A three-dimensional computational SCS and a nerve fiber model were used to determine the effect of the lateral distance between two leads at the same vertebral level T8 and the effect of the addition of anodes with two parallel leads at T8 and three different lateral distances on the model-based results (perception thresholds, activated DC fiber area and depth, and position of the first stimulated fiber).

Results: With two parallel leads programmed with symmetrical polarities, the maximal DC fiber area stimulated was found for a lateral distance of 5 mm. The results also show a higher preference for DR stimulation as the lateral distance increased. The addition of positive contacts at the same level of active contacts in the second lead produces a displacement of the first stimulated fiber laterally.

Conclusions: A lateral distance of 5 mm shows a DC stimulated fiber area greater than when leads are placed contiguously. The addition of anodes creates an effect whereby the area of paresthesia is not displaced to the midline, but in the opposite direction. This may be useful when the leads are too close and stimulation of one of the sides is compromised.

Keywords: Computational model, dorsal column stimulation, dorsal root stimulation, polarity, spinal cord stimulation

INTRODUCTION

Spinal cord stimulation (SCS) has been used to treat chronic severe pain based on the delivery of a current through electrodes placed on the epidural space. The first SCS implant was performed by Shealy et

al[1] in 1967, based on the mechanism of action pro-posed by Melzack and Wall[2] in 1965, known as the gate control theory. This theory postulates that the activation of Aβ fibers in the dorsal column (DC) inhibits the C fibers responsible for pain transmission and produces a sensation of paresthesia in the stimulated Aβ fibers. According to this mechanism, the paresthesia (and consequently the stimulation of the corresponding dermatomes) must entirely cover the patient's painful area[3–5]. Although in some patients, paresthesia coverage does not assure pain relief [6,7], most computational studies investigating the effect of tonic SCS (ie, whose mechanism of action is based on the creation of action potential in large axons, contrary to subthreshold modes of stimulation) are aimed at finding programming strategies maximizing the activated DC fibers' area. [8–11]

The analysis of lead location in the function of the area of paresthesia desired from a population of patients treated with neurostimulation therapy can be found in several studies,[6,12–14] as well as the effect of the programmable parameters of the electrical

pulse.[15,16] In addition to clinical observations, mathematical models of SCS have been used to determine optimal lead position, polarity programming, and parameters of stimulation, among others. The first study showing the use of numerical methods, like the finite element method (FEM) to solve differential equations governing the behavior of the electric field in electrical stimulation of the spinal cord, was performed by Coburn et al.[17,18] Holsheimer,[19] Struijk et al,[20] and Manola and Holsheimer[21] developed their own FEM program for the analysis of the effect of lead geometry, polarity, and pulse parameters. Other groups developed similar simulation models based on the FEM, with an increasing number of elements and subsequently less computing error as computer hardware capabilities increased.[8,9,22–26] Recently, some personal- ized models based on the magnetic resonance imaging (MRI) of a patient have been developed.[27,28]

To optimize the effect of paresthesia-based SCS, it is important to maximize the area of DC fibers stimulated (A_{DC}, in mm^2)[6] to assure coverage of all the dermatomes affected. The effective area and location of the stimulated DC fibers depend on many parameters, such as device choice (number and geometry of the leads implanted), the position of the leads in the epidural space, the programming parameters of the electrical pulses (amplitude, polarity, and pulse width, among others), and the anatomy of the patient. The effect of some of these parameters has been investi- gated by computational modeling.[8–10]

In this study, we focused on two clinical-related aspects of the therapy: the optimal lateral distance between two parallel leads to maximize the paresthesia area and the effect of the transverse stimulation (addition of anodes in the parallel lead) in the position of this area. For this research, we assume the best polarities for the SCS in complex pain deduced in our previous article,[9] ie, guarded cathode (GC [consists of one positive contact followed by a negative contact and a positive contact in the same lead +−+]) and dual guarded cathode (DGC [consists of one positive contact followed by two negative contacts and a positive contact in the same lead +−−+]). To the best our knowledge, there are no previous works analyzing these important factors. To compare the effect of these parameters, we studied their influence on the A_{DC}, the threshold amplitude to stimulate fibers in the DCs and DRs, and the position of the first stimulated fiber (FSF). The primary goal was the paresthesia coverage of the pain area, even if it means a sensation of paresthesia in non-pain areas, and consequently, our first parameter of optimization was the A_{DC}. When increasing the amplitude once the first fiber is stimulated at the threshold amplitude, the fibers around this first fiber are recruited, as well as fiber with lower diameter. Therefore, we considered the position of the

FSF important for the optimal coverage and focus of the paresthesia. The research was then focused on the tonic stimulation for complex pain using two parallel leads implanted at the same vertebral level, T8.

MATERIALS AND METHODS

Our simulation model has been previously presented,[9] and it is based on two other submodels. One is a three-dimensional (3D) model of the spinal cord, called the volume conductor model, which incorporates the main anatomic structures of the spine (bone, epidural fat, dura mater, cerebrospinal fluid, dorsal roots [DRs], and white and gray matter) as well as two octopolar leads with two different geometries (intercontact distance [ICD], in mm) and positions (lateral distance between both), as shown in Figure 1a,b. It uses realistic dimensions obtained from MRI images of 15 healthy adult volunteers[29] and includes the tissue electrical properties published by different authors,[30–32] as shown in Table 1. A computer numerical software program (COMSOL Multiphysics version 5.3, COMSOL Inc, Burlington, MA) based on the FEM solves the differential equations providing the electric field in the volume. The volume conductor model uses an adaptative mesh of tetrahedral quadratic elements with approximately two million nodes and around 1.6 million elements with size from 0.067 to 1.57 mm.

The FEM is used for the calculation of the electrical distribution as an approximate solution of the Laplace equation:

$$\nabla^2 V = 0$$

The current density J (x, y, z) is obtained from the generalized version of Ohm's law:

$$J = \sigma \times E$$

$$E = -\nabla V_e$$

where V_e is the electrical potential of a specific point of the volume conductor model; E, the electric field; J, the current density; and σ, the electrical conductivity tensor. V_e, E, and J are calculated using the conjugate gradient iterative method solver considering a quasi- static problem.[33] The boundary conditions of the problem are the zero current in the limits of the volume conductor and the user-defined voltage in the lead's contacts. Because the impedance is constant (it only changes during the first weeks after the implant and then remains constant[34]), there is no difference between talking about current or voltage because they are lineally linked by Ohm's law.

The electric potential in the points of interest was used to study the action potential behavior in the fibers, using a self-developed program[9] based on the Richardson, McIntyre, and Grill fiber model[35] and implemented with MATLAB R2018a (MathWorks, Natick, MA). This model solves the following equation of the membrane potential in each Ranvier node V_n, considering the value of the electrical potential V_e previously obtained from Equation (3), using the modeling of the axon shown in Figure 1c:

$$\frac{dV_n}{dt} = \frac{1}{C_{m,n}}\left[-I_{ion,n} + G_{axial}\left(V_{n-1} - 2V_n + V_{n+1} + V_{e,n-1} - 2V_{e,n} + V_{e,n+1}\right)\right]$$

where *n* is the Ranvier node number, C_m is the membrane capacitance, I_{ion} is the sum of ionic currents crossing the membrane at the node n, and G_{axial} is the conductance between the center of two adjacent compartments. This model determines whether a fiber, under the external electric field previously calculated, creates an action potential. The distance between Ranvier nodes was set to 100 times the outer fiber diameter.[36]

According to Feirabend et al,[37] the largest nerve fiber near the DC midline of the spinal cord is 12.8 µm in diameter. Despite the low density of the 12.8-µm diameter fibers in the DC, we assumed that this fiber is first recruited in SCS, because larger fibers present a lower stimulation threshold than smaller ones.[38] Because experimental geometric parameters are available for the 12.8-µm

diameter axons, we included 4000 of these fibers in the DC area to reduce the effect of the fibers' position, even though we knew that this density is not real. In a strict sense, we should refer to the area where a fiber with a 12.8-µm diameter or more is stimulated, rather than the A_{DC}. This unrealistic fiber's distribution is adopted to find results applicable in a general point of view while being conscient that they could present differences with individual patients, mainly in the perception threshold in DC fibers and the position of the fibers stimulated.

Within this study, we computed the evolution of key parameters from the results of our mathematical model, such as the perception threshold in DCs (PT_{DC}), the lowest voltage needed to activate the first DC nerve fiber with a 12.8-µm diameter; the perception threshold in DRs (PT_{DR}), the lowest voltage needed to activate the first DR nerve fiber with a 15-µm diameter in our model[38,39]; the recruitment ratio, the ratio between both ($R_{DC/DR}$ = PT_{DC}:PT_{DR}), where lower ratios suppose a bigger preference for DC stimulation with respect to DR stimulation; the maximum transversal area (in mm^2) of the DCs within which DC nerve fibers are activated at the simulation amplitude (A_{DC}); and the position of the FSF in the DC relative to the anatomic midline, by definition of the perception threshold, at PT_{DC} amplitude. All the simulations were performed at T8 level. A more detailed description of each parameter and how each is calculated can be found in our previous article.[9] The stimulation pulse consisted of a monophasic perfect rectangular wave with a 300-µs duration. The pulses were monophasic, defining the cathode as the negative electrode and the anode as the positive one. The stimulation was produced close to the cathode because the anodic stimulation needs an amplitude five to eight times higher than the cathodic stimulation.[40] We selected the 300-µs pulse duration because it was the default pulse duration in some commercial devices and it was used in our previous research works.[9,28] It is critical to maintain the pulse width for all the con- figurations studied because the parameters calculated depend on this value.[8] The amplitude of the simulation for calculating A_{DC} was

1.4 times the lower PT_{DC} or PT_{DR}, assuming the hypothesis of the discomfort threshold (maximal amplitude the patient can perceive without making the paresthesia painful) by Barolat[14] or Howell et al.[41] The relation between the discomfort and the perception threshold (1.4) cannot be calculated by the mathematical model, so we selected the value most used by many authors, based on clinical observation.[8,10,42,43]

Lateral Distance

The parameters provided by the model were evaluated for different lateral distances between leads, from 2 to 10 mm center to center (Fig. 1b), with increments of 1 mm, to determine the lateral distance that shows the maximal stimulated DC fibers. GC and DGC polarities (Fig. 2) were analyzed in two types of lead: one with 4 mm of ICD and another with 1 mm of ICD (Fig. 1b), with 3 mm of contact length and 1.3 mm of contact diameter.

In this study, we used two programs (number 1 and number 2) in the sense of Aló et al[44] or the channels by North et al,[13] as different pulse generators delivering electric waves at same amplitudes and symmetric polarities with respect to the midline, simultaneously or sequentially. Based on our clinical practice, each program has the

cathodes defined in only one lead to control the paresthesia in each side, as shown in Figure 3 (program number 1 stimulates from the left lead, and program number 2 stimulates from the right lead). Because the leads are placed perfectly at the same lateral distance to the midline, the amplitude of the simulation was the same for both programs.

Transverse Stimulation

The term transverse stimulation is usually used when three contacts at the same rostrocaudal level are used,[45–47] but this configuration requires three percutaneous leads or a surgical paddle, whereas the use of two percutaneous parallel leads is the most common setting in our practice. Therefore, the concept of transverse stimulation is also used with two leads implanted, when different polarity contacts are used in each lead, creating an electric field going from one lead to the other. The effect of the addition of anodes at the same vertebral level was analyzed because it is one of the tools used to move the stimulation area laterally after the implant once the leads are fixed. We studied the effect of the transverse stimulation in all the parameters evaluated in the model, including the position of the FSF. A new parameter was introduced, the second derivative of the potential field in the direction of the DC fibers ($\Delta^2V/\Delta Z^2$). This last parameter represents the area of preferred stimulation because it is close to the activation function described by Rattay[48] and is used to determine the fibers stimulated.[25] From our experience, this parameter provides valuable qualitative information but does not negate the need for a fiber model to determine whether a fiber is stimulated. The FSF is at the maximum parameter $\Delta^2V/\Delta Z^2$, showing how this position is not intuitive and needs a mathematical calculus to be determined. Two polarities were considered: the DGC, adding one to four anodes at the same level of the contacts, which provides five different polarities in total (Fig. 2a), and the GC, adding one to three anodes, resulting in four different polarities (Fig. 2b). These combinations were studied for lateral distances (center to center) of 2, 4, and 6 mm at the T8 level, with 4-mm ICD leads. In total, nine polarities were considered at three different distances, resulting in 27 simulations.

RESULTS

Lateral Distance

The effect of the lateral distance between two parallel leads, from 2 to 10 mm (center to center) with 1-mm increments, was studied on the stimulation characteristics. Because these configurations are most used in our clinical practice for complex pain (when few dermatomes are affected, such as

in failed back surgery syndrome), we studied the results for the 4-mm and 1-mm ICD leads, and our most used polarities, DGC (Fig. 3a) and GC (Fig. 3b). The sum of the DC fiber area stimulated is only valid when using two symmetric and simultaneous programs (program number 1 and program number 2), with the cathodes in each lead, as shown in Figure 3.

The A_{DC} created by one lead and two leads and the overlapping area, as shown in Figure 4, varied with the lateral distance between the leads, with an ICD of 4 mm (DGC, Fig. 5a; GC, Fig. 5b) and with an ICD of 1 mm (DGC, Fig. 5c; GC, Fig. 5d). As shown in Figure 5, the A_{DC} created by one lead decreased when each lead became more lateral, except for that at 1 mm of ICD and GC polarity (Fig. 5d). The overlapping area follows the same tendency. Because the total stimulated area is the sum of the areas created by each lead (twice the area of one lead) minus the overlapping area, the effect of the distance between the leads on the stimulated area presents a maximum value for 5 mm between leads, for all ICD and polarities studied. It is also noted that DGC polarity stimulates a higher area

than GC polarity, as shown in Figure 5a,c (DGC polarity) compared

with Figure 5b,d (GC polarity). DR stimulation is a limiting factor when the stimulation of many dermatomes is searched (such as in failed back surgery syndrome pathology) because the discomfort threshold could be reached with the stimulation of only one or a few dermatomes corresponding to the DR fibers, avoiding the coverage of all the desired areas of pain.[42,43,49] This is why, even if the DGC produces the largest A_{DC}, as shown in Figure 5a,c compared with Figure 5b,d, GC polarity could be a good choice if DR stimulation is prematurely reached.[9] Under these circumstances of DR stimulation with DGC polarity, the choice of GC stimulation could be indicated.

To explain the effect of the overlapping area, we selected two configurations: the last distance analyzed presenting an over- lapping area (8 mm, Fig. 4a) and the leads very close (2 mm, Fig. 4c). The area of overlap for 8 mm of lateral distance was very small (0.4 mm^2) (Fig. 4a), and the sum of the areas (3.0 mm^2) was approximately double each (1.7 mm^2), resulting in a total A_{DC} of 2.8 mm^2. In contrast, for a lateral distance of 2 mm, the area stimulated by each lead was higher (2.7 mm^2), but the overlapping area was also high (2.4 mm^2), causing a total A_{DC} of 3.1 mm^2 (Fig. 4c). Combining these opposite effects of the lateral distance, the maximum total area created by both leads was a compromise found for a lateral distance of 5 mm (Fig. 4b). For this separation, the area created by each lead was 2.2 mm^2, less than the area created by each lead with 2 mm of separation, but the overlapping area was 1.1 mm^2, and the total area was 3.3 mm^2, the maximum determined for the separations studied. A similar effect can be seen for the GC polarity.

Although the parameter of optimization chosen in our analysis is

the total A_{DC}, there are other factors concerning the shape of the DC fibers stimulated. It seems convenient to ensure a band of stimulated fibers along the shallowest layer of the DC at the level of the cathodes, to be able to stimulate the wider DC area and reach the paresthesia objective. To evaluate this characteristic, which is difficult to quantify, we defined the minimum depth of the DC area stimulated as the lower depth of the DC fibers stimulated, ie, the distance between the deepest fiber stimulated and the pia mater. A minimum depth of zero means that there is an area of DC fibers in the shallowest layer where no DC fibers are stimulated (Fig. 3b). The area of no stimulation shown in Figure 3b appears when the overlapping area is zero.

When studying the effect of the lateral distance on PT_{DC}, PT_{DR}, and the recruitment ratio $R_{DC/DR}$, the model shows that the values of PT_{DC} remained constant when the distance between the leads increases for all configurations (Fig. 6a–d), ie, for both ICD and polarities studied. However, in

general, PT_{DR} decreased when the distance between the leads increased; therefore, $R_{DC/DR}$ also increased. PT_{DR} showed a maximum value of 9.4 V for a 3-mm lateral distance (GC and 4-mm ICD, Fig. 6b), and this value decreased dramatically when the distance increased until a value of

3.8 V for a lateral distance of 10 mm, showing the preference for DR stimulation increases when the leads are separated. In addition, the results indicate that GC polarity showed superiority in terms of avoiding DR stimulation for lateral distances between leads >6 mm (Fig. 6b,d), but with lower DC fiber area stimulated (Fig. 5b,d). In contrast, for greater distances between the leads (approximately 10 mm), $R_{DC/DR}$ showed greater preference for DR stimulation with GC polarity than with DGC polarity (Fig. 5b,d compared with Fig. 5a,c),

because of a significant decrease in PT_{DR} when the distance augments. For the 1-mm ICD, we obtained from the model a significantly higher value for PT_{DR} for all distances and consequently a lower $R_{DC/DR}$, demonstrating a lower preference for DR stimulation for the 1-mm ICD leads than with the 4-mm ICD, at the cost of a lower DC fiber area stimulated (Figs. 6d and 5d).

Transverse Stimulation

The effect of the addition of anodes, in a lead parallel to the stimulation lead and at the same vertebral level, was studied. The different polarities of the stimulation electrodes are shown in Figure 2a,b. The addition of a cathode contralateral to the anodes (ie, in a parallel lead at the same rostrocaudal level as shown in Fig. 2) is called transverse stimulation, although this denomination is used more frequently when using three parallel leads, creating a guarded tripole in the lateral direction.[47,50] To add anodes is a strategy when the area of paresthesia must be moved laterally.

For this study, two 4-mm ICD leads (parallel and laterally separated by 2, 4, and 6 mm center to center) were considered. For each of these three distances, DGC polarity and GC polarity were used, first without any added anode and subsequently with anodes in the other lead added (up to four or three configurations for the DGC and GC cases, respectively). We abbreviated the polarities as DGC + number of added anodes or GC + number of added anodes, as shown in Figure 2.

There was similar behavior for all configurations, even if some polarities showed particularities in the results of the calculated parameters. These parameters were, as in previous cases, PT_{DC}, PT_{DR}, $R_{DC/DR}$, A_{DC}, and a new parameter, the position of the FSF in the DC. We also calculated the area and distribution of the stimulated DC fibers for the case of the largest displacement of the FSF. It is possible to conclude from the computed values that the effects of the addition of anodes in the studied parameters (displacement of the FSF, thresholds, and DC area stimulated) were higher when the leads were closer. Therefore, the maximum effect was determined at 2 mm of lateral separation between the leads. In Figure 7a, an explanation of the concept of the displacement of the FSF is shown. The addition of anodes induced a displacement of the FSF from its position (Fig. 7b,c). The parameter shown is the distance between the FSF with added anodes, compared with the position with all the contacts in only one lead (GC and DGC polarities, Fig. 2). A positive value depicts a displacement in the direction of the lead with the anodes added, ie, moving the FSF laterally, whereas a negative value means a displacement to the

midline (Fig. 7a).

In 25 of the 27 cases, we noted an increase in the distance between the midline and the position of the FSF as the anodes were added (positive displacement), and we surmised that the FSF was

displaced from the midline through the position of additional anodes (Fig. 7b,c). This effect was maximal with anodes contralateral to cathodes (DGC + 2 and GC + 1) and at the minimum lateral distance (2 mm). The maximal displacement obtained (0.87 mm) corresponded to DGC + 2 polarity with leads separated by 2 mm. For the GC starting polarity, the maximum was found with GC + 1 polarity (0.58 mm), also at 2 mm. Considering the size of the spine, this displacement of the FSF may be enough to change the stimulated dermatomes when increasing the amplitude.

In terms of PT_{DC} and PT_{DR}, the variation was similar for DGC and GC polarities (Fig. 7d–g). The perception thresholds (PT_{DC} and PT_{DR}) increased when one additional anode was used and decreased when two, three, or four additional anodes were used. The addition of anodes induced a decrease in the area compared with the polarity with all the contacts in one lead only (DGC and GC)

(Fig. 7h,i). For DGC polarity, the minimum area resulted when two anodes were added, except in the case of 2 mm of lateral distance, where the minimum area was, with one added anode, 1.99 to 1.28 mm^2, 2.29 to 1.51 mm^2, and 2.71 to 2.17 mm^2 for 6, 4, and 2 mm of lateral separation, respectively (Fig. 7h). The behavior of the stimulated area after adding the anodes for GC polarities was similar, but with marginal differences, and a minimum for one added anode: 1.04 to 0.91 mm^2, 1.34 to 1.11 mm^2, and 1.37 to 1.24 mm^2 for 6, 4, and 2 mm of lateral separation, respectively (Fig. 7i). As noted, the A_{DC} values were higher when the leads were closer.

We analyzed the variations of the area of stimulation for trans- verse polarity at the configurations with larger displacement of the FSF, for DGC + 2 and GC + 1 (Fig. 2) at the three distances studied, as shown in Figures 8 and 9, respectively. These figures show the position of the FSF and the distribution of the A_{DC} (left and right) for each lateral separation (2, 4, and 6 mm) with DGC polarity (first row of boxes, Fig. 8), GC polarity (first row of boxes, Fig. 9), the same calculated parameters for DGC + 2 polarity (second row of boxes, Fig. 8), GC + 1 polarity (second row of boxes, Fig. 9), and the previously described second derivative of the potential field in the direction of the DC fibers ($\Delta^2V/\Delta Z^2$) for DGC + 2 polarity (third row of boxes, Fig. 8) and GC + 1 polarity (third row of boxes, Fig. 9) for each lateral separation. As already explained, the DC area decreased in the three cases, and not only was the FSF displaced, but also the distribution of the DC fibers stimulated in each side varied noticeably. With leads separated by 2 mm, and DGC polarity, the distribution between the ipsilateral and contralateral areas varied from 59% to 41% to 79% to 21%, respectively (Fig. 8). For 4 and 6 mm, the contralateral area almost disappeared when adding the anodes (we consider ipsilateral/contralateral the same/opposite side to the active lead, the lead with the cathodes). For GC polarity, the effect of the addition of one anode contralateral to the cathode (GC + 1, Fig. 2b) was similar, changing from a 58% to 42% distribution in the ipsilateral/contralateral side, respectively, to 77% to 23% for a lateral distance of 2 mm, and almost disappearing with the contralateral DC fibers stimulated for a lateral distance of 4 and 6 mm (Fig. 9).

DISCUSSION

Our results suggest that the optimal lateral distance between the leads is 5 mm and that the addition of anodes in the second lead creates an effect contrary to what might be assumed intuitively and was published[51]; the area of paresthesia is not displaced to the midline, but in the opposite direction.

Our simulations are based on the use of two leads at the same rostrocaudal level, parallel to the

midline and programmed with symmetric independent programs controlling each side independently, as performed in our clinical practice. There is no generally accepted guideline regarding the use of cathodes in only one of the leads (when two parallel leads are used) or both, leaving this decision to the criterion of the programmer. Our choice is to separate the paresthesia field for each side, programming only cathodes in one lead per program, to facilitate amplitude control of each side by the patient with their patient programmer, as previously explained.

Lateral Distance

One consideration while implanting two lead electrodes is that the lateral distance affects the position of the stimulated DC fibers in the epidural space. The rostrocaudal level of the lead is defined by the dermatomes to be stimulated during the intraoperative test, but the lateral position must be determined, as should the lateral distance between the leads when two leads are used. There is no criterion for this distance; some physicians place their lead contiguously[52,53] and others more distantly. To the best of our knowledge, there is no study determining the best lateral distance between parallel leads. The results of our simulations are valid for the same configurations used by our group for treating complex bilateral pain (like back and leg pain). This configuration implies placing the leads at the same vertebral level (not staggered), parallel to the midline and symmetric with respect to it (as close as possible to this desired placement because the lead position depends on anatomic characteristics on each patient), and programming two symmetric programs, each with the cathodes in only one lead, as per other studies.[54,55] We do not use cathodes in both leads in the same program because we prefer to control the paresthesia in each side separately by means of two simultaneous programs, each preferably controlling only one side.

The maximum lateral distance between leads is usually limited by the DR stimulation because if the leads are placed too lateral, the preference of DR stimulation increases, as we can see with the variation of $R_{DC/DR}$ with the laterality of the lead. In contrast, if both leads are closer to the midline, the possibility of DR stimulation is remote, but the total area of stimulation is not optimal. Furthermore, the difficulty to distinguish each side stimulated by each lead could be high, resulting in the possibility of stimulating the same side with both leads, because the anatomic and physiologic midline do not have to coincide.

According to our results, a lateral distance of 5 mm between leads (center to center) is a safe distance regarding DR stimulation and to maximize the A_{DC}, both for 1- and 4-mm ICD. The differences of DC fiber area stimulated are not dramatic from 2- to 5-mm lateral distance with DGC polarity (from 3.1 mm^2 with contiguous leads to 3.3 mm^2 for 5-mm lateral distance with the 4-mm ICD lead). With GC polarity, this difference is higher (1.0 mm^2 for 2-mm distance to 1.6 mm^2 for 5-mm distance with the 1-mm ICD lead). In terms of DC fiber stimulated area, our results suggest that there is no reason to place the leads with >5 mm of separation center to center, as the area decreases and the possibility of DR stimulation increases.

Transverse Stimulation: Lateral Displacement of the FSF

We analyzed the possibility of lateral displacement of the DC fiber stimulation area once the leads are fixed (for example in successive programming sessions) and, consequently, the area of paresthesia from one side of the body to the other one. It is important to modify the area of

paresthesia after implantation when needed because it is impossible to move the leads to improve coverage of the paresthesia. As explained, there is a widespread idea that adding positive poles in the second lead (while the anodes are in the first lead) moves the stimulated fiber in the DC to this lead, ie, to the midline,[51] because it seems intuitive that the area of DC fiber stimulation depends on the shape of the electric field. There are studies analyzing the superiority of the transverse tripole in SCS.[50,56] This configuration requires that three parallel leads are implanted, or a surgical paddle lead is used. We expect that the position of the FSF (the first fiber stimulated at the perception threshold amplitude) could be a good indicator of the area of paresthesia raising the amplitude to the discomfort threshold. The effect of the addition of anodes in the second lead is to displace the FSF in the opposite direction to the second lead. This effect is attributable to the fact that the area of preferred stimulation is not defined by the electric field (which moves to the midline adding anodes), but by the second difference of the electric potential field in the rostrocaudal direction (represented in the volume conductor model by the second axial derivative of the electrical potential[48,57,58]).

Even if the addition of anodes in the second lead (also known as transversal stimulation) creates a nonintuitive opposite effect, moving the A_{DC} further lateral could be an effective tool in some situations. The displacement of the DC stimulated area in a lateral direction is an objective in many cases when programing a neurostimulator once the leads are placed and cannot be moved. There is no map of DC fibers to determine where to move the stimulated DC fiber area according to the desired paresthesia area, and the final polarity is based on the patient response to different configurations. The effect of this addition of anodes is more significant as the leads are closer. Feirabend et al,[37] based on the study by Smith and Deacon,[59] have proposed a distribution of the DC fibers associated with each dermatome at T10–T11 level, and Holsheimer[54] has considered this to show the importance of moving the A_{DC} laterally. In fact, these studies show the need for a somatosensory atlas of paresthesia areas at DC level for more precise placement of the leads, based nowadays on clinical observation.[60]

Model Limitations

The use of simulations based on mathematical models implies a simplification that must be considered. This simplification affects the geometry of the spine because it is built from an average of many patients[29] and can show important discrepancies for individual cases. Besides, the volume conductor model is built from a spine slide (different for each vertebra) and does not consider anatomic particularities as stenosis.

Another important point is the unrealistic position of the leads, parallel to the midline, and the fact that the anatomic midline matches the physiologic midline. It is important to note that this ideal lead placement is a choice of our group, because other implanters prefer a non–midline-parallel orientation of the leads.[52,53]

Finally, another important limitation of the mathematical models is the lack of clinical validation. In the case of the parameters studied in this research (lateral distance between leads and polarity options), there are no clinical data using these parameters as variables. Further clinical research in this field would be desirable.

CONCLUSIONS

The use of computational models is a time- and cost-saving tool for the optimization of technical parameters.[61] For dual lead placement at the same rostrocaudal level implants, a lateral separation of 5 mm between the leads showed the maximal DC fiber area stimulated according to our model. Because the difference between 2 and 5 mm of lateral separation was low, and for >5 mm, the possibility of stimulating DR increases, this range from 2 to 5 mm seems to be a good election for the placement of the leads. The addition of anodes contralateral to the cathodes when using two parallel leads could be a good strategy to move the area of stimulation laterally, but the effect is the nonintuitive opposite: The FSF is displaced laterally far of the midline, instead of to the midline. This effect could be useful when two leads are used in proximity and stimulating one side is a problem: Programming anodes contralateral to the cathodes moves the stimulation area to the side and promotes DR stimulation in some cases. Our modeling study provides guidance for improving outcome in the programming strategies for patients, but clinical testing should be necessary to extrapolate our laboratory results.

REFERENCES

1. Shealy CN, Mortimer JT, Reswick JB. Electrical inhibition of pain by stimulation of the dorsal columns: preliminary clinical report. Anesth Analg. 1967;46:489–491.
2. Melzack R, Wall PD. Pain mechanisms: a new theory. Science. 1965;150:971–979.
3. Jensen MP, Brownstone RM. Mechanisms of spinal cord stimulation for the treatment of pain: still in the dark after 50 years. Eur J Pain. 2019;23:652–659.
4. Caylor J, Reddy R, Yin S, et al. Spinal cord stimulation in chronic pain: evidence and theory for mechanisms of action. Bioelectron Med. 2019;5:1–41.
5. Holsheimer J, Barolat G. Spinal geometry and paresthesia coverage in spinal cord stimulation. Neuromodulation. 1998;1:129–136.
6. He J, Barolat G, Holsheimer J, Struijk JJ. Perception threshold and electrode position for spinal cord stimulation. Pain. 1994;59:55–63.
7. Smits H, van Kleef M, Holsheimer J, Joosten EAJ. Experimental spinal cord stimu- lation and neuropathic pain: mechanism of action, technical aspects, and effec- tiveness. Pain Pract. 2013;13:154–168.
8. Lee D, Hershey B, Bradley K, Yearwood T. Predicted effects of pulse width pro- gramming in spinal cord stimulation: a mathematical modeling study. Med Biol Eng Comput. 2011;49:765–774.
9. Durá JL, Solanes C, De Andrés J, Saiz J. Computational study of the effect of electrode polarity on neural activation related to paresthesia coverage in spinal cord stimulation therapy. Neuromodulation. 2019;22:269–279.
10. Manola L, Holsheimer J, Veltink P. Technical performance of percutaneous leads for spinal cord stimulation: a modeling study. Neuromodulation. 2005;8:88–99.
11. Holsheimer J, Struijk JJ, Wesselink WA. Effects of electrode configuration and geometry on fiber preference in spinal cord stimulation. Annu Int Conf IEEE Eng Med Biol Proc. 1996;1:343–344.
12. Oakley J, Varga C, Krames E, Bradley K. Real-time paresthesia steering using continuous electric field adjustment. Part I: intraoperative performance. Neuro- modulation.

2004;7:157–167.
13. North RB, Ewend MG, Lawton MT, Piantadosi S. Spinal cord stimulation for chronic, intractable pain: superiority of “multi-channel” devices. Pain. 1991;44:119–130.
14. Barolat G. Epidural spinal cord stimulation: anatomical and electrical properties of the intraspinal structures relevant to spinal cord stimulation and clinical correla- tions. Neuromodulation. 1998;1:63–71.
15. Abejón D, Cameron T, Feler C, Pérez-Cajaraville J. Electric parameters optimization in spinal cord stimulation. Study in conventional nonrechargeable systems. Neu- romodulation. 2010;13:281–286 [discussion: 286–287].
16. Abejõn D, Rueda P, Del Saz J, Arango S, Monzõn E, Gilsanz F. Is the introduction of another variable to the strength-duration curve necessary in neurostimulation? Neuromodulation. 2015;18:182–190.
17. Coburn B, Sin WK. A theoretical study of epidural electrical stimulation of the spinal cord— part I: finite element analysis of stimulus fields. IEEE Trans Biomed Eng. 1985;32:971–977.
18. Coburn B. A theoretical study of epidural electrical stimulation of the spinal cord— part II: effects on long myelinated fibers. IEEE Trans Biomed Eng. 1985;32:978–986.
19. Holsheimer J. Computer modelling of spinal cord stimulation and its contribution to therapeutic. Spinal Cord. 1998;36:531–540.
20. Struijk JJ, Holsheimer J, Barolat G, He J, Boom HBK. Paresthesia thresholds in spinal cord stimulation: a comparison of theoretical results with clinical data. IEEE Trans Rehab Eng. 1993;1:101–108.
21. Manola L, Holsheimer J. Technical performance of percutaneous and laminectomy leads analyzed by modeling. Neuromodulation. 2004;7:231–241.
22. Hernández-Labrado GR, Polo JL, López-Dolado E, Collazos-Castro JE. Spinal cord direct current stimulation: finite element analysis of the electric field and current density. Med Biol Eng Comput. 2011;49:417–429.
23. Mørch CD, Nguyen GP, Wacnik PW, Andersen OK. Mathematical model of nerve fiber activation during low back peripheral nerve field stimulation: analysis of electrode implant depth. Neuromodulation. 2014;17:218–225.
24. Capogrosso M, Wenger N, Raspopovic S, et al. A computational model for epidural electrical stimulation of spinal sensorimotor circuits. J Neurosci. 2013;33:19326– 19340.
25. Arle JE, Carlson KW, Mei L, Shils JL. Modeling effects of scar on patterns of dorsal column stimulation. Neuromodulation. 2014;17:320–333.
26. Zhang TC, Janik JJ, Grill WM. Mechanisms and models of spinal cord stimulation for the treatment of neuropathic pain. Brain Res. 2014;1569:19–31.
27. Lempka SF, Zander HJ, Anaya CJ, Wyant A, Ozinga JG, Machado AG. Patient-spe- cific analysis of neural activation during spinal cord stimulation for pain. Neuro- modulation. 2020;23:572–581.
28. Solanes C, Durá JL, A´ ngeles Canós M, De Andrés J, Martí-Bonmatí L, Saiz J. 3D patient-specific spinal cord computational model for SCS management: potential clinical applications. J Neural Eng. 2021;18:036017. https://doi.org/10.1088/1741- 2552/abe44f.
29. Fradet L, Arnoux PJ, Ranjeva JP, Petit Y, Callot V. Morphometrics of the entire human spinal cord and spinal canal measured from in vivo high-resolution anatomical magnetic resonance

imaging. Spine (Phila Pa 1976). 2014;39:E262–E269.
30. Wesselink WA, Holsheimer J, Boom HBK. Analysis of current density and related parameters in spinal cord stimulation. IEEE Trans Rehabil Eng. 1998;6:200–207.
31. Struijk JJ, Holsheimer J, Boom HBK. Excitation of dorsal root fibers in spinal cord stimulation: a theoretical study. IEEE Trans Biomed Eng. 1993;40:632–639.
32. Huang Q, Oya H, Flouty OE, et al. Comparison of spinal cord stimulation profiles from intra- and extradural electrode arrangements by finite element modelling. Med Biol Eng Comput. 2014;52:531–538.
33. Bossetti CA, Birdno MJ, Grill WM. Analysis of the quasi-static approximation for calculating potentials generated by neural stimulation. J Neural Eng. 2008;5:44–53.
34. Abejon D, Feler CA. Is impedance a parameter to be taken into account in spinal cord stimulation? Pain Physician. 2007;10:533–540.
35. Richardson AG, McIntyre CC, Grill WM. Modelling the effects of electric fields on nerve fibres: influence of the myelin sheath. Med Biol Eng Comput. 2000;38:438– 446.
36. Wesselink WA, Holsheimer J, Nuttin B, et al. Estimation of fiber diameters in the spinal dorsal columns from clinical data. IEEE Trans Biomed Eng. 1998;45:1355– 1362.
37. Feirabend HKP, Choufoer H, Ploeger S, Holsheimer J, Van Gool JD. Morphometry of human superficial dorsal and dorsolateral column fibres: significance to spinal cord stimulation. Brain. 2002;125:1137–1149.
38. Holsheimer J. Which neuronal elements are activated directly by spinal cord stimulation. Neuromodulation. 2002;5:25–31.
39. McIntyre CC, Richardson AG, Grill WM. Modeling the excitability of mammalian nerve fibers: influence of afterpotentials on the recovery cycle. J Neurophysiol. 2002;87:995–1006.
40. Holsheimer J. Principles of neurostimulation. In: Simpson BA, ed. Electrical Stimu- lation and the Relief of Pain. Elsevier Health Sciences; 2003:18–36.
41. Howell B, Lad SP, Grill WM. Evaluation of intradural stimulation efficiency and selectivity in a computational model of spinal cord stimulation. PLoS One. 2014;9: e114938.
42. Bradley K. The technology: the anatomy of a spinal cord and nerve root stimulator: the lead and the power source. Pain Med. 2006;7(suppl 1):S27–S34.
43. Holsheimer J, Buitenweg JR. Review: bioelectrical mechanisms in spinal cord stimulation. Neuromodulation. 2015;18:161–170.
44. Aló KM, Yland MJ, Charnov JH, Redko V. Multiple program spinal cord stimulation in the treatment of chronic pain: follow-up of multiple program SCS. Neuro- modulation. 1999;2:266–272.
45. Rana MV, Knezevic NN. Tripolar spinal cord stimulation for the treatment of abdominal pain associated with irritable bowel syndrome. Neuromodulation. 2013;16:73–77.
46. Holsheimer J, Struijk JJ, Wesselink WA. Analysis of spinal cord stimulation and design of epidural electrodes by computer modeling. Neuromodulation. 1998;1:14– 18.
47. Sankarasubramanian V, Buitenweg JR, Holsheimer J, Veltink P. Triple leads programmed to perform as longitudinal guarded cathodes in spinal cord stimulation: a modeling study. Neuromodulation. 2011;14:401–410 [discussion: 411].
48. Rattay F. Analysis of models for external stimulation of axons. IEEE Trans Biomed Eng.

1986;33:974–977.
49. Levy RM. Anatomic considerations for spinal cord stimulation. Neuromodulation. 2014;17(suppl 1):2–11.
50. Oakley JC, Espinosa F, Bothe H, et al. Transverse tripolar spinal cord stimulation: results of an international multicenter study. Neuromodulation. 2006;9:192–203.
51. Oakley JC, Prager JP. Spinal cord stimulation: mechanisms of action. Spine (Phila Pa 1976). 2002;27:2574–2583.
52. Aló KM, Redko V, Charnov J. Four year follow-up of dual electrode spinal cord stimulation for chronic pain. Neuromodulation. 2002;5:79–88.
53. Van Buyten JP, Van Zundert J, Milbouw G. Treatment of failed back surgery syn- drome patients with low back and leg pain: a pilot study of a new dual lead spinal cord stimulation system. Neuromodulation. 1999;2:258–265.
54. Holsheimer J. Does dual lead stimulation favor stimulation of the axial lower back? Neuromodulation. 2000;3:55–57.
55. Aló KM. Lead positioning and programming strategies in the treatment of complex pain. Neuromodulation. 1999;2:165–170.
56. Sankarasubramanian V, Buitenweg JR, Holsheimer J, Veltink P. Performance of transverse tripoles vs. longitudinal tripoles with anode intensification (AI) in spinal cord stimulation: computational modeling study. Neuromodulation. 2014;17:457– 463 [discussion: 463–464].
57. Zierhofer CM. Analysis of a linear model for electrical stimulation of axons— critical remarks on the “activating function concept.”. IEEE Trans Biomed Eng. 2001;48:173–184.
58. Ladenbauer J, Minassian K, Hofstoetter US, Dimitrijevic MR, Rattay F. Stimulation of the human lumbar spinal cord with implanted and surface electrodes: a computer simulation study. IEEE Trans Neural Syst Rehabil Eng. 2010;18:637– 645.
59. Smith MC, Deacon P. Topographical anatomy of the posterior columns of the spinal cord in man. The long ascending fibres. Brain. 1984;107:671–698.
60. Barolat G, Massaro F, He J, Zeme S, Ketcik B. Mapping of sensory responses to epidural stimulation of the intraspinal neural structures in man. J Neurosurg. 1993;78:233–239.
61. Capogrosso M, Lempka SF. A computational outlook on neurostimulation. Bio- electron Med. 2020;6:10.

FIGURES

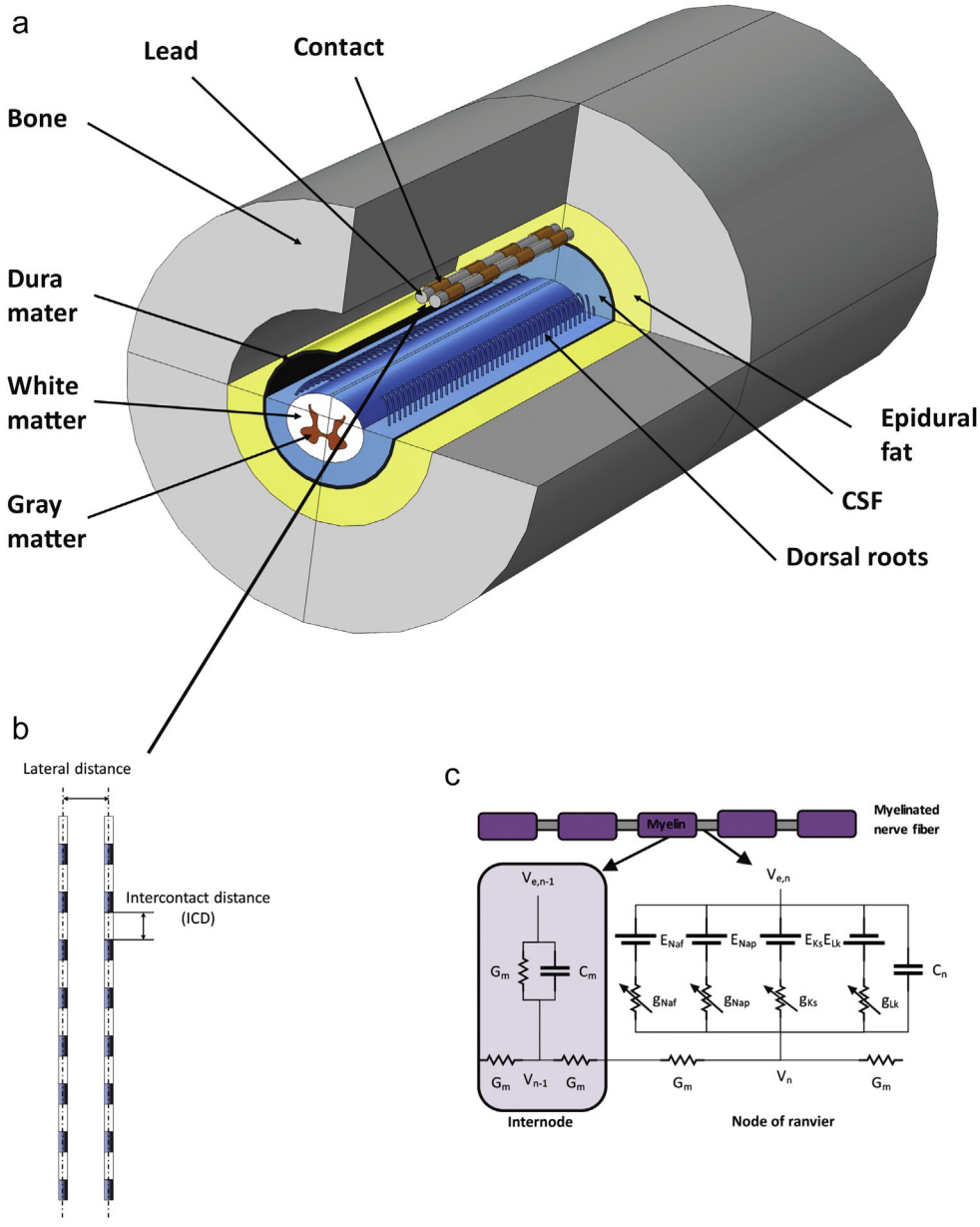

Figure 1. a. 3D volume conductor model. b. ICD and lateral distance between the leads. c. Fiber model. CSF, cerebrospinal fluid.

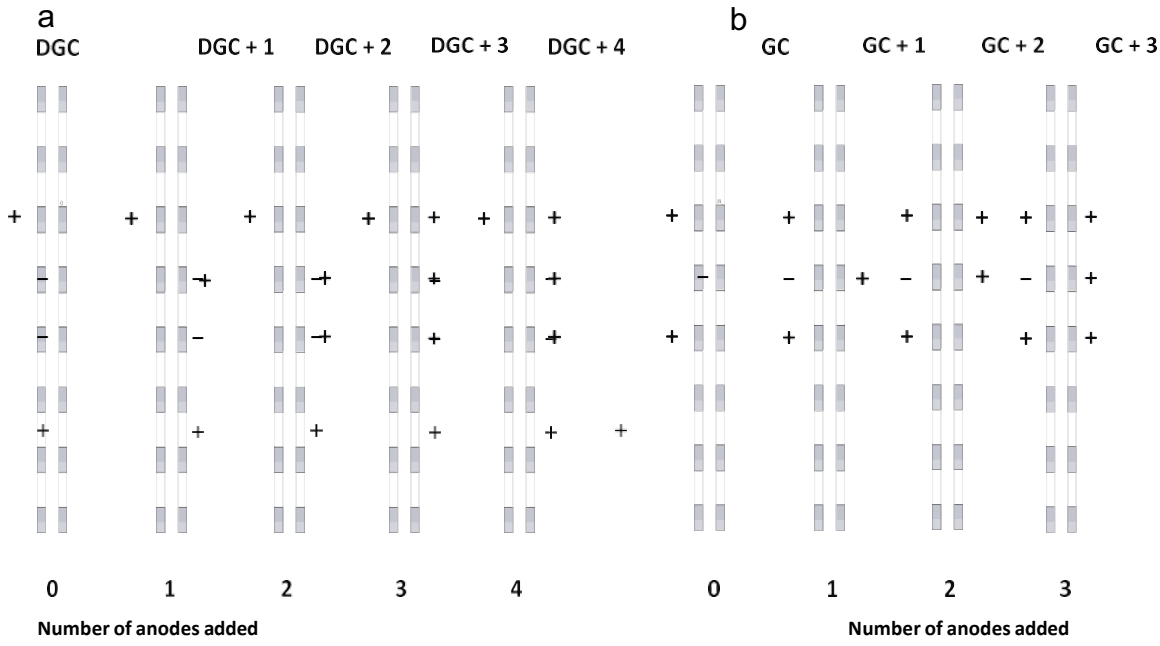

Figure 2. Transverse polarities from (a) DGC polarity and (b) GC polarity.

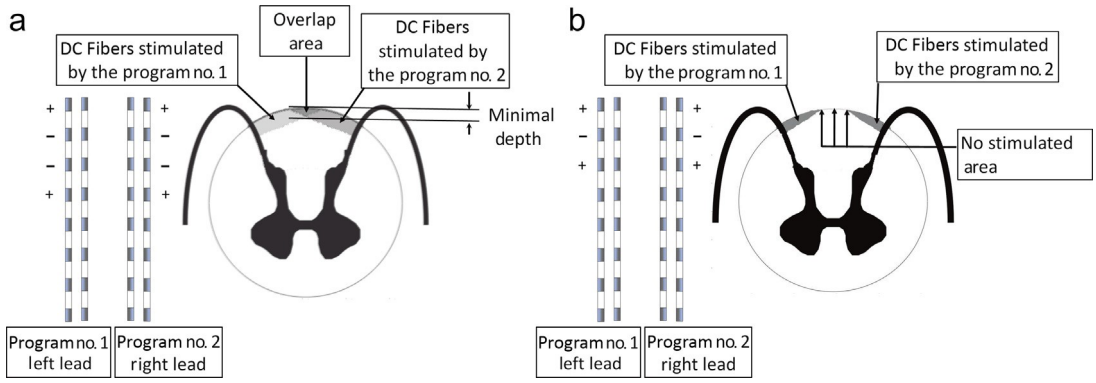

Figure 3. A_{DC} by each program (1 and 2) and total, with all the cathodes in only one lead per program. a. Leads at 4 mm axis to axis and DGC polarity. b. Leads at 10 mm axe to axe and GC polarity.

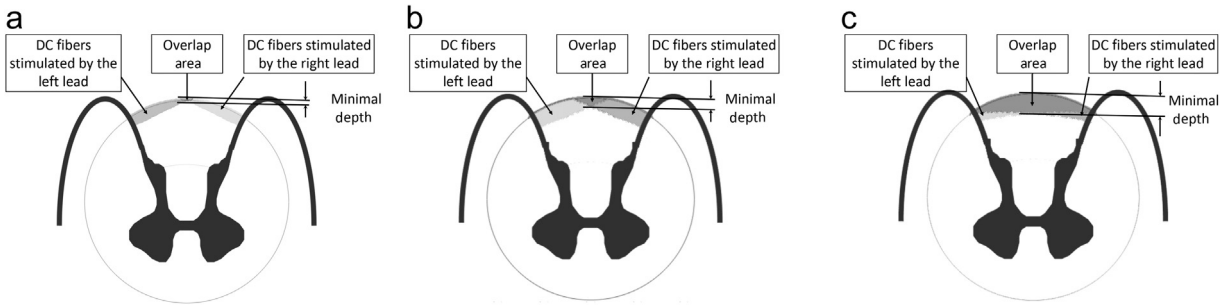

Figure 4. Spinal cord axial image of DC fibers stimulated with two leads, DGC polarity, and 4-mm ICD, separated by (a) 8 mm, (b) 5 mm, and (c) 2 mm.

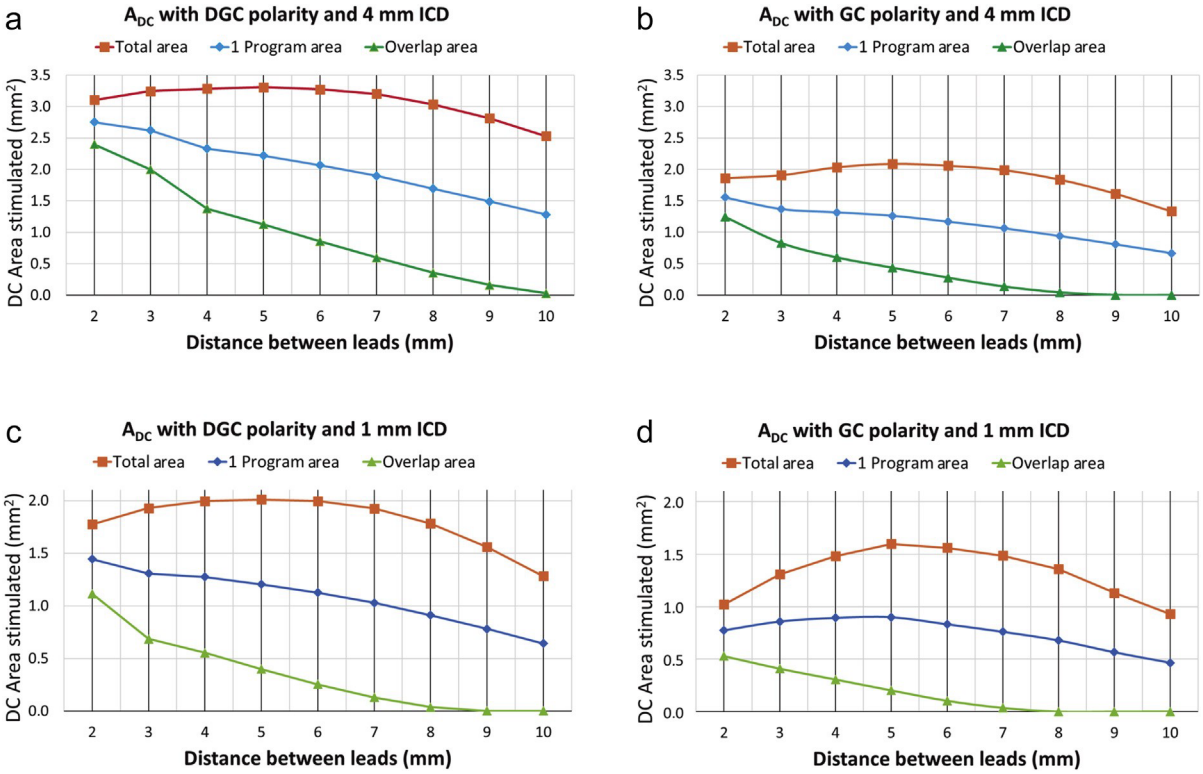

Figure 5. Effect of the lateral distance between the two parallel leads programmed symmetrically on the A_{DC} by one program, two symmetrical programs, and overlapped area of both programs for (a) DGC and 4-mm ICD, (b) GC and 4-mm ICD, (c) DGC and 1-mm ICD, and (d) GC and 1-mm ICD.

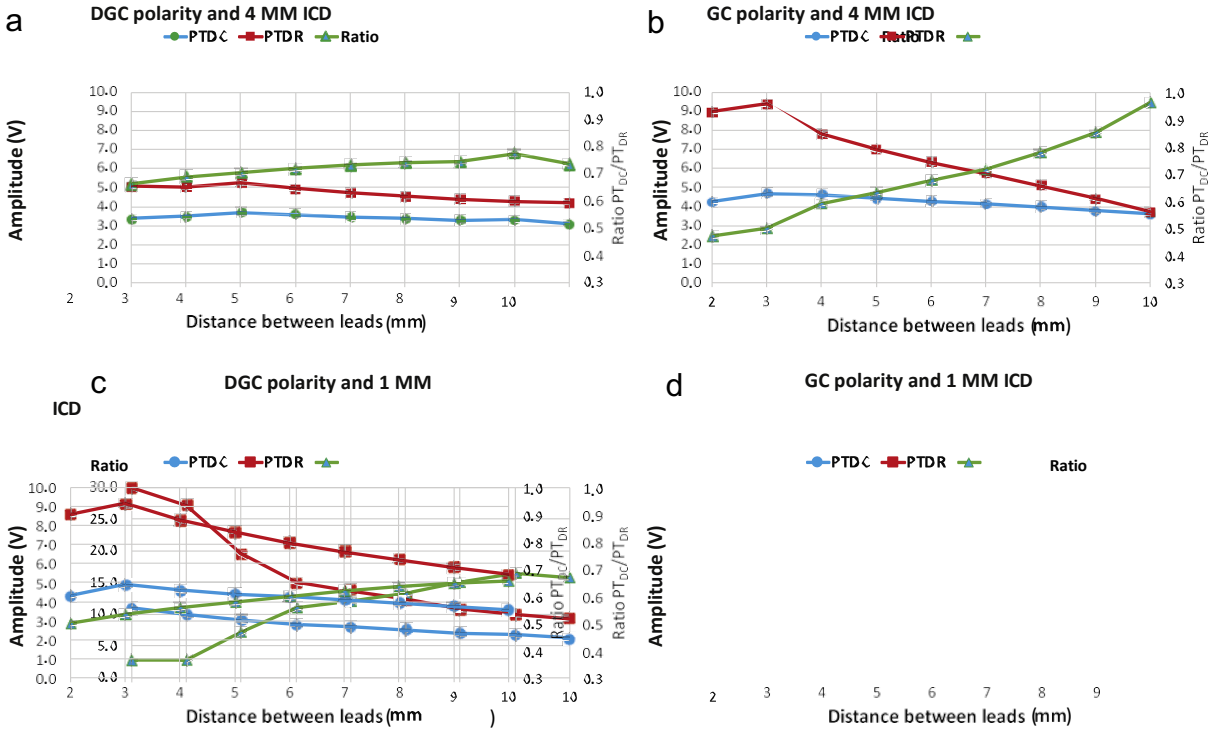

Figure 6. Effect of the lateral distance between the two parallel leads programmed symmetrically on the PT_{DC}, PT_{DR}, and $R_{DC/DR}$ for 4-mm ICD with (a) DGC polarity,

(b) GC polarity, (c) 1-mm ICD with DGC polarity, and (d) GC polarity (note that the maximal amplitude value is different for the [d] figure).

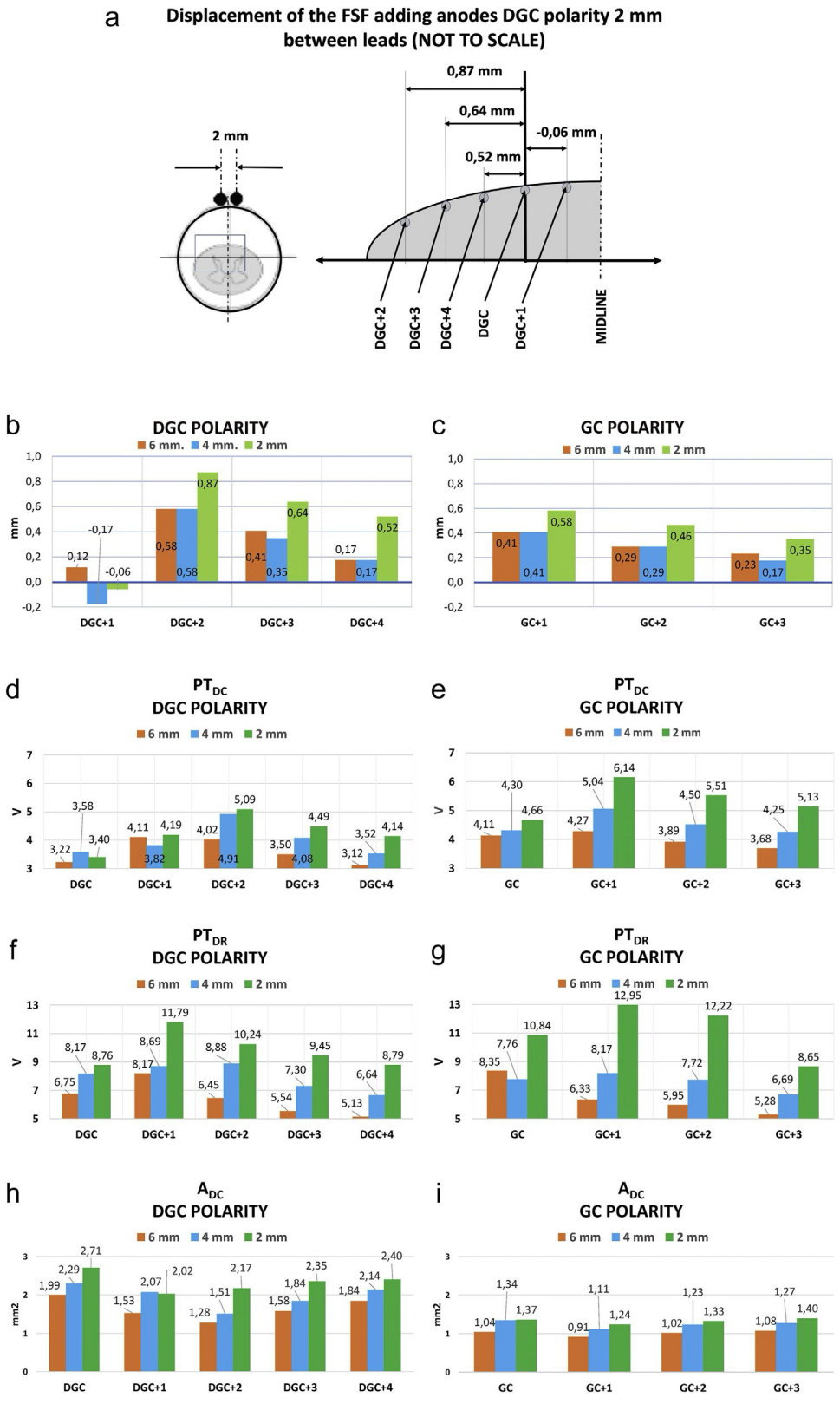

Figure 7. (a) Scheme of the displacement of the FSF concept and effect of the addition of anodes (positive contacts) in the second lead at the same level of a lead polarity at a lateral distance of 2, 4, and 6 mm on the displacement of the FSF with (b) DGC and (c) GC, (d and e) on the PT_{DC} fibers, (f and g) on the PT_{DR} fibers, and (h and i) on the A_{DC}.

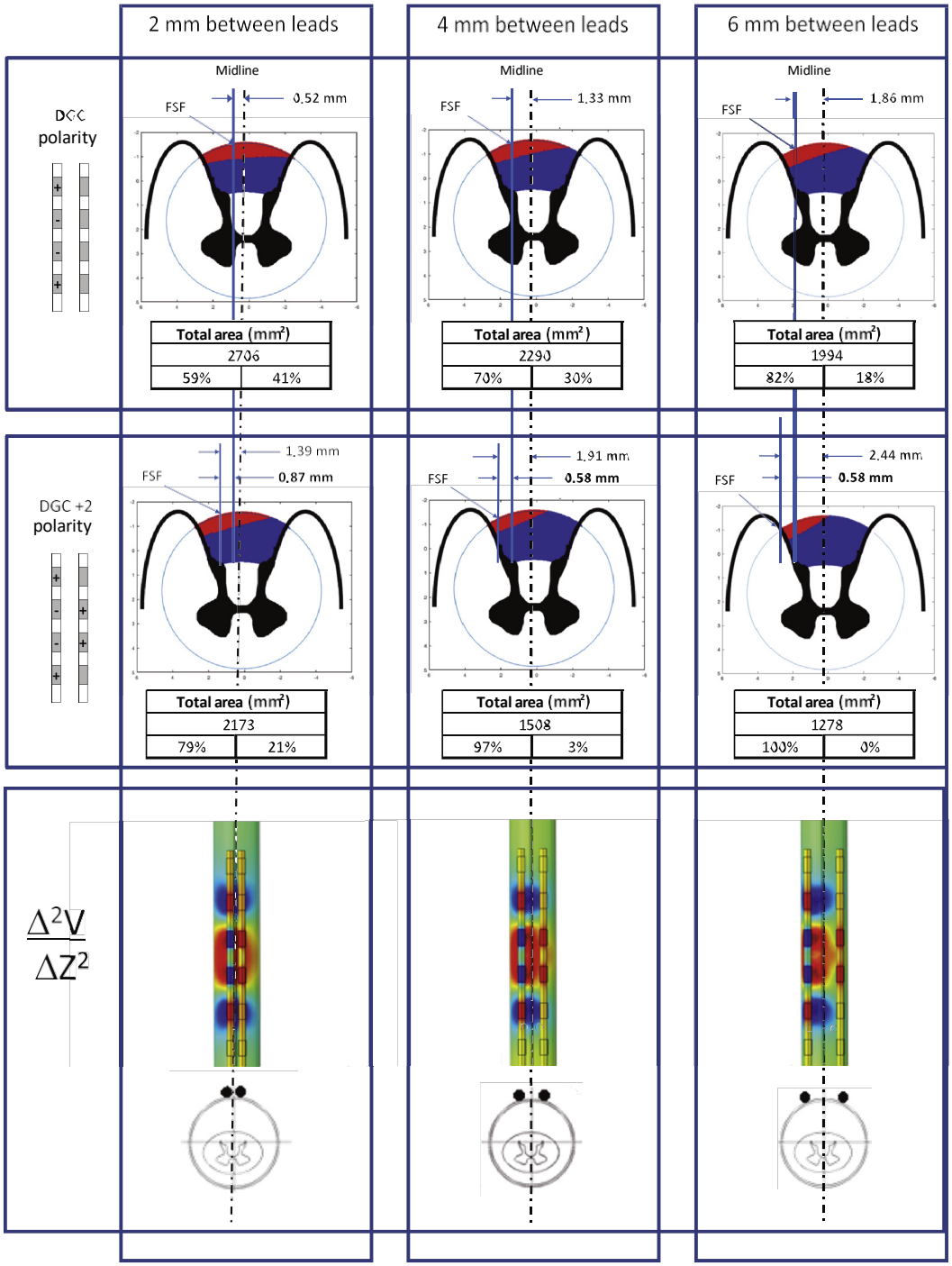

Figure 8. Effect of the addition of two anodes in the second lead at the same level of the cathodes of a lead with DGC polarity at a lateral distance of 2, 4, and 6 mm on the position of the FSF, the A_{DC} total and in each side, and the second derivative of the electric potential in the rostrocaudal direction.

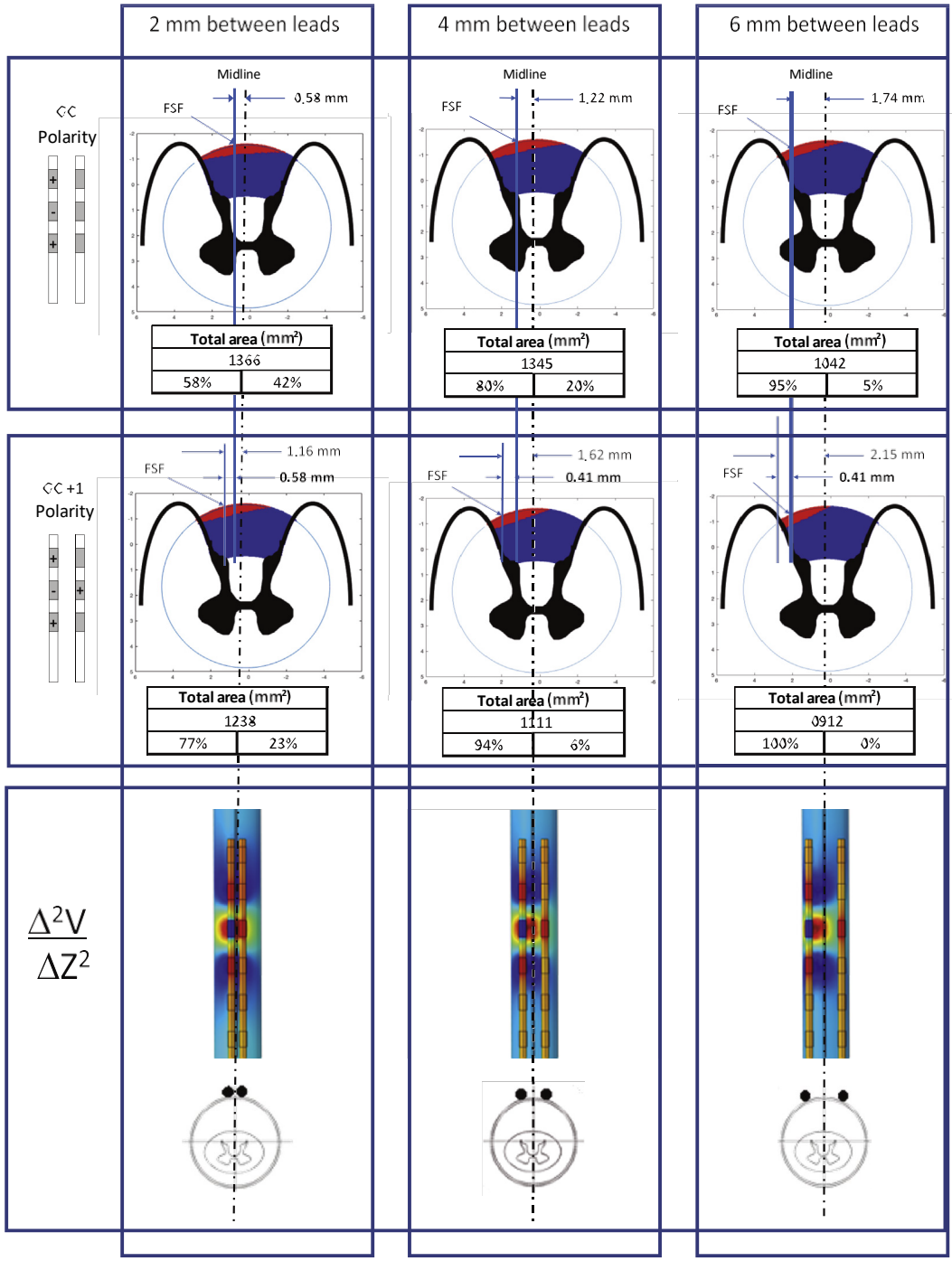

Figure 9. Effect of the addition of two anodes in the second lead at the same level of the cathodes of a lead with GC polarity at a lateral distance of 2, 4, and 6 mm on the position of the FSF, the A_{DC} total and in each side, and the second derivative of the electric potential in the rostrocaudal direction.

Table 1. Conductivities Considered in the Volume Conductor Model.

Material	Electrical conductivity (S/m)
Gray matter	0.230
White matter transversal	0.083
White matter longitudinal	0.600
Cerebrospinal fluid	1.700
Dura mater	0.030
Fat	0.040
Bone	0.020
Lead's contact (platinum-iridium alloy)	5.28×10^6
Lead's insulation	0.002
Electrode-tissue interface	0.150